

Microcavity polaritonlike dispersion doublet in resonant Bragg gratings

Fabio Biancalana,¹ Leonidas Mouchliadis,² Celestino Creatore,³ Simon Osborne,⁴ and Wolfgang Langbein²

¹Max Planck Institute for the Science of Light, Günther-Scharowsky-Str. 1/Bau 24, 91058 Erlangen, Germany

²School of Physics and Astronomy, Cardiff University, The Parade, CF24 3AA Cardiff, United Kingdom

³Department of Physics "A. Volta," Università degli Studi di Pavia, via Bassi 6, Pavia I-27100, Italy

⁴Tyndall National Institute, Lee Maltings, Prospect Row, Cork, Ireland

(Received 30 July 2009; published 17 September 2009)

Periodic structures resonantly coupled to excitonic media allow the existence of extra intragap modes ("Braggoritons") due to the coupling between Bragg photon modes and bulk excitons. This induces unique dispersive features, which can be tailored by properly designing the photonic band gap around the exciton resonance. We report that Braggoritons realized with semiconductor gratings have the ability to mimic the dispersion of quantum-well microcavity polaritons. This gives rise to peculiar nonlinear phenomena, such as slow-light-enhanced nonlinear propagation and an efficient parametric scattering at two "magic frequencies."

DOI: [10.1103/PhysRevB.80.121306](https://doi.org/10.1103/PhysRevB.80.121306)

PACS number(s): 71.35.Gg

Since the pioneering proposals by Yablonovitch and John,¹ photonic crystals (PhCrS), structures characterized by a spatially periodic dielectric function, have attracted enormous attention due to their rich physics. In particular, the occurrence of photonic band gaps (PBGs), i.e., frequency regions where the propagation of light is strongly inhibited and the extraordinary ability to manipulate and control the photonic flow, make PhCrS very appealing for many applications.¹ Furthermore, the current accurate engineering of photonic states allows us to investigate light-matter phenomena in PhCrS, with one of the most fascinating being the strong-coupling regime of light-matter interaction. Nontrivial modifications of the photonic dispersion are expected to occur when PBG materials are coupled to polarizable excitonic media²⁻⁷ since in this case the true eigenmodes of the mixed photonic-excitonic system are exciton-polaritons,⁸ i.e., the normal modes born from the strong coupling between Wannier-Mott excitons and Bragg photons propagating in the PBG structure.

In this Rapid Communication, we show through theoretical analysis that, by embedding a three-dimensional (3D) exciton resonance within the PBG of a one-dimensional (1D) Bragg grating, the dispersion relation of the resulting exciton-polariton states can, under certain conditions, mimic the dispersion of a *doublet* of microcavity (MC) polaritons, i.e., the quasiparticles arising from the coupling between two-dimensional excitons in a quantum well and the optically confined photons in a semiconductor planar microcavity.⁸ The very peculiar dispersion features of these Bragg polariton modes give rise to a wide variety of nonlinear phenomena, absent in standard gratings, such as slow-light-enhanced nonlinear propagation and an ultra-efficient parametric scattering at two magic frequencies. In addition, owing to the extremely small effective mass of these hybrid exciton-photon modes, routes for the appearance of macroscopic coherence in solid-state systems are opened.

Following a procedure similar to the one used in Ref. 9 in the context of conventional nonresonant Bragg gratings, and extending it to include both the forward and the backward exciton polarization waves, it is possible to derive the following *polaritonic coupled-mode equations* (PCMEs) written in dimensionless units:

$$i[\partial_\tau + \tilde{\gamma}_{\text{ph}}]f + i\partial_z f + \kappa b + p_f/2 = 0, \quad (1)$$

$$i[\partial_\tau + \tilde{\gamma}_{\text{ph}}]b - i\partial_z b + \kappa f + p_b/2 = 0, \quad (2)$$

$$i\partial_\tau p_f + (i\tilde{\gamma}_x + d)p_f + [|p_f|^2 + 2|p_b|^2]p_f + \rho f = 0, \quad (3)$$

$$i\partial_\tau p_b + (i\tilde{\gamma}_x + d)p_b + [|p_b|^2 + 2|p_f|^2]p_b + \rho b = 0, \quad (4)$$

In Eqs. (1)–(4), the fields $\{f, b\}$ represent the amplitude of the slowly varying envelopes of the forward and the backward propagating electric fields, respectively, while $\{p_f, p_b\}$ are the corresponding quantities for the exciton polarization field. Spatial dispersion terms have been omitted for simplicity, as their contribution to the propagation dynamics is negligible. The dimensionless temporal and longitudinal spatial variables are $\tau \equiv t/t_0$ and $\zeta \equiv z/z_0$, respectively, with $t_0 \equiv \epsilon_b/\omega_0$ and $z_0 \equiv ct_0/\sqrt{\epsilon_b}$, with ϵ_b being the average background dielectric function of the grating and ω_0 being the central pulse frequency. The 1D grating is described by the dielectric function $\epsilon(z) = \epsilon_b \{1 + \mu [e^{ik_B z} + e^{-ik_B z}]/2\}$, where $\mu \ll 1$ is the depth of the grating and $k_B \equiv 2\sqrt{\epsilon_b}\omega_0/c$ is the grating Bragg wave number. The dimensionless frequency detuning between the Bragg frequency ω_B and the exciton resonant frequency ω_x is given by $d \equiv \Delta\omega t_0$, where $\Delta\omega = \omega_B - \omega_x$. The linear absorptions of the background medium γ_{ph} and the exciton oscillator damping γ_x (i.e., the exciton homogeneous linewidth) are also considered in our model through the dimensionless quantities $\tilde{\gamma}_{\text{ph},x} \equiv t_0 \gamma_{\text{ph},x}$. The polariton splitting ω_c , which measures the interaction between the transverse components of the excitonic polarization and the retarded electromagnetic field, is specified by the dimensionless parameter $\rho \equiv t_0 \omega_c^2 / (2\omega_x)$. Finally, solution of the linearized equations (1)–(4) yields the dispersion relation of Bragg polaritons $\delta = \delta(q)$, where $\delta \equiv \Delta\omega/\omega_0$ and $q \equiv \Delta k/k_0$ are the frequency and the wave-number detunings from the band-gap center, respectively, and have been introduced via a phase shift of the fields of the kind $\exp(iq\zeta - i\delta\tau)$. It is important to note that in our system the source of the Kerr-type nonlinearity is provided by the repulsive exciton-exciton (XX) interactions encoded in the cubic terms in Eqs. (3) and (4).¹⁰

Throughout this Rapid Communication we use a design based on zinc oxide (ZnO) as a representative example of our theoretical calculations. ZnO has received substantial attention in recent years due to the robustness of its exciton reso-

nances, which remain stable up to room temperature and its exceptionally large binding energy and oscillator strength.¹¹ Following recent advances in ZnO growth and deposition, clean exciton resonances have been produced using molecular-beam epitaxy,¹² pulsed-laser deposition,⁴ sputtering,¹³ and led to the realization of a ZnO MC.⁴ We use ZnO as our excitonic material [see also Fig. 3(e)], and we therefore design the photonic crystal in order to have the PBG located around ω_x . The second kind of layer is made of ZrO_2 . The free exciton binding energy of ZnO is $\hbar\omega_c \approx 60$ meV, and the exciton central frequency is $\hbar\omega_x \approx 3.3771$ eV, which corresponds to $\lambda_x \approx 367.4$ nm.¹² The linear absorption coefficient and the exciton homogeneous linewidth of ZnO depend considerably on the fabrication technique. However, at $T=5$ K we make the estimates $\gamma_{\text{ph}} \approx 2.5$ meV and $\gamma_x \approx 0.25$ meV.¹⁴ The strength of the exciton-photon coupling is regulated by $\rho/t_0 = \omega_c^2/(2\omega_x) \approx 5.33 \times 10^{-4}$ eV. Since $\hbar\omega_c > \gamma_{x,\text{ph}}$, the physical conditions for achieving strong-coupling regime are met. Near the exciton transition frequency, ZnO has a refractive index $n_1 \approx 2.37$, while for ZrO_2 $n_2 \approx 2.326$ at the same wavelength. Thus we have the following grating parameters, to be used in Eqs. (1)–(4): $\mu = \Delta n^2/\epsilon_b \approx 0.0187$ and $\kappa = \mu\epsilon_b/4 \approx 0.0258 \ll 1$, satisfying the shallow grating condition on which our PCMEs are based. The quarter-wavelength condition gives the layers' widths $L_1 = 38.8$ nm and $L_2 = 39.9$ nm for ZnO and ZrO_2 , respectively. The spatial nonlocal response of excitons (considered in Ref. 6) is not relevant here since (i) the modifications in the exciton mass induced by the weak confinement (see, e.g., Ref. 8) are small and (ii) the folding of the band structure due to the periodicity greatly reduces the effects of spatial dispersion for large momenta. The nonlinear refractive index of ZnO at λ_x is estimated to be $n_{\text{NL}}(\text{ZnO}) \approx 10^{-11}$ m²/W at 5 K, which is about nine orders of magnitude larger than that of bulk silica.¹⁵

Equations (1)–(4) represent the foundational result of this Rapid Communication. Previous attempts to describe polaritonic gratings have been made in the framework of the linear transfer-matrix method,² approaches that do not take into account the large nonlinear optical response of excitons near resonance, or by using a model based on Maxwell-Bloch equations,¹⁶ but without taking into account the crucial importance of both forward and backward propagating exciton polarization waves.

Figures 1(a)–1(c) show the evolution of the coupled and bare linear dispersions when varying d from vanishing to negative values. Coherent coupling between 3D bulk excitons and Bragg photons gives rise to two intragap modes (Bragg polaritons or Braggoritons²), the dispersion of which can be efficiently tailored by simply tuning d , for instance, by slightly modifying the grating parameters around the fixed exciton resonant frequency.

The four branches in question [which we label upper- and lower-photon (UP,LP) and upper- and lower-Bragg-oriton (UB,LB) branches; see Figs. 1(a)–1(c)] have a striking resemblance with the dispersions of a doublet of coupled MC polaritons.¹⁷ As shown in Fig. 1(c) for a detuning $d = -0.04$, the pair (UP,LP) form the first half of the doublet (named MC1), while its counterpart (named MC2), formed by the pair (LP,UB), is reversed, and not placed symmetrically with

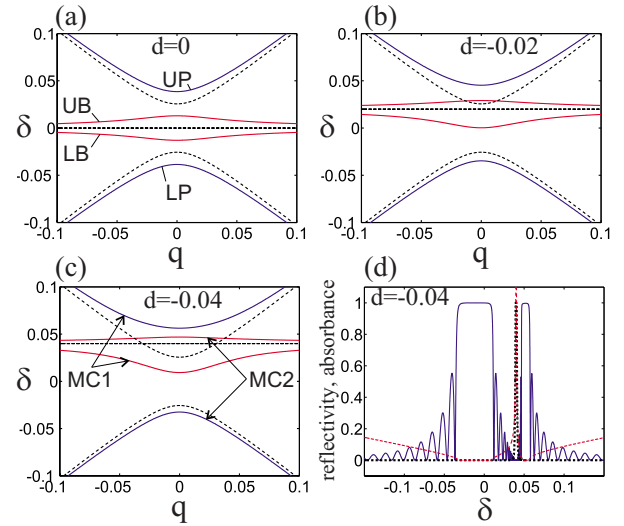


FIG. 1. (Color online) (a)–(c) Polariton dispersion on the (δ, q) plane for three different values of d . Dashed lines are the bare Bragg photon and exciton dispersions. Blue solid (dark gray) lines indicate upper-photon (UP) and lower-photon (LP) branches; red solid (light gray) lines are upper-Bragg-oriton (UB) and lower-Bragg-oriton (LB) branches. (d) Reflectivity R_j in blue solid (dark gray) line and absorbance A_j in black dotted line as functions of δ for a finite grating ($L = 14 \mu\text{m}$ for our proposed ZnO design). The dispersion is shown with red dashed (light gray) lines.

respect to MC1 for $d \neq 0$. As mentioned above, the condition of strong exciton-photon coupling is realized for both MC1 and MC2. Note that, by using the formalism based on coupled-mode theory [Eqs. (1)–(4)], one can accurately describe only regions well inside the first Brillouin zone and in the proximity of the central Bragg frequency of one specific band gap only.⁹ An analysis that goes beyond the coupled-mode theory approximation in multilayer systems can be found in Ref. 6. However, the nonlinear effects originating from XX interactions, which are the focus of our Rapid Communication, are not discussed in the latter work.

Equations (1)–(4) allow calculation of the linear reflectivity R_j and absorbance A_j as functions of δ for finite gratings [see Fig. 1(d)]. Physical dispersion branches are selected with the criterion $R \leq 1$ [see also Fig. 2(a)]. It is evident that the polariton feature introduces an *anomalous transmittance* region located inside the band gap, at a detuning d from the band-gap center, which divides the band gap into two smaller subband gaps.² Furthermore, we observe here that the formation of such subgaps is accompanied by the appearance of *two zero group-velocity dispersion (GVD) points*, therefore dividing the spectrum into alternating regions of anomalous [$(\partial^2 q_j / \partial \delta^2) < 0$] and normal [$(\partial^2 q_j / \partial \delta^2) > 0$] GVD [see dots in Figs. 2(a) and 2(b)]. It is worth noticing that *in conventional gratings such points do not exist*, while MC polaritons possess only one inflection point on their lower branch, which is of paramount importance for the occurrence of the nonlinear effects observed in experiments.^{17,18} We shall see that the full significance of this analogy goes well beyond the mere similarity in the dispersive properties.

Due to its large excitonic component and flat dispersion, the UB (LB) branch with $d < 0$ ($d > 0$) turns out to be a

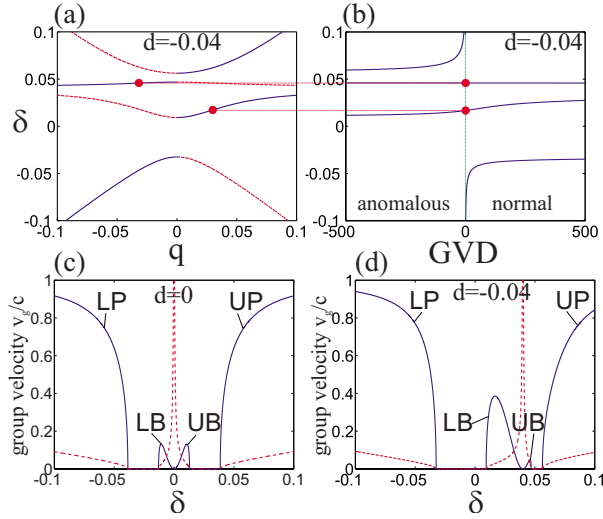


FIG. 2. (Color online) (a) Physical parts of the dispersion branches [for which $R(\delta) \leq 1$] are indicated with blue solid (dark gray) lines, for $d = -0.04$. Red (light gray) dots indicate the position of the two inflection points on the UB and LB branches, which are located at q 's that have the same magnitude but opposite signs, see also [Fig. 3(b)]. (b) GVD ($\partial^2 q_j / \partial \delta^2$) as a function of δ . Red (light gray) dots indicate zero-GVD points. (c) and (d) Solid blue (dark gray) lines are the group velocities $v_{g,j}/c = (\partial q_j / \partial \delta)^{-1}$ as functions of q , for $d = 0$ and $d = -0.04$, respectively. Red dashed (light gray) lines indicate the dispersion.

potential candidate for slow-light-enhanced nonlinear optics at low intensities.¹⁹ This is confirmed by calculating the group velocities (GVs) of all branches for $d = 0$ and $d = -0.04$ [Figs. 2(c) and 2(d), respectively]. The UP and LP branches show GVs approaching the speed of light in the medium [normalized to ± 1 in Figs. 2(c) and 2(d)] for large values of δ , as in conventional gratings. The GV can be reduced considerably when δ approaches the band edges, but then progressively less photons will be available due to evanescence of the electric field in those regions.¹⁹ However, Figs. 2(c) and 2(d) show that, in the proximity of the UB and LB branches ($\delta \sim d$), small GVs can be obtained. For $d = 0$ [Fig. 2(c)] the central GV curve is symmetric, while, for $d \neq 0$, the GV curve is asymmetric [see Fig. 2(d)]. Figures 2(c) and 2(d) are in qualitative agreement with the experimental measurements performed in similar structures, e.g., see Fig. 3(b) in Ref. 3. Close to $\delta \approx d$, exciton absorption can strongly affect both UB and LB branches, depending on the precise value of $\tilde{\gamma}_x$. Being mostly excitonic in nature and spectrally narrower, the UB (LB) branch is the one most affected by exciton absorption for $d < 0$ ($d > 0$). Moreover, a reduction in group velocity comes at the price of a reduced bandwidth, which is a fundamental limitation for all slow-light devices.¹⁹ This corresponds here to the progressive straightening of the flat UB branch for large values of $|d|$. At low temperatures, typically $T < 5$ K, there are frequency regions for which absorption is reasonably small and relatively far from the band edges, where the group velocity is greatly reduced. For instance, Fig. 2(d) shows that an increase in the group index up to 20 is achieved for realistic parameters corresponding to the ZnO-based grating structure discussed above. By increasing the interaction time between the me-

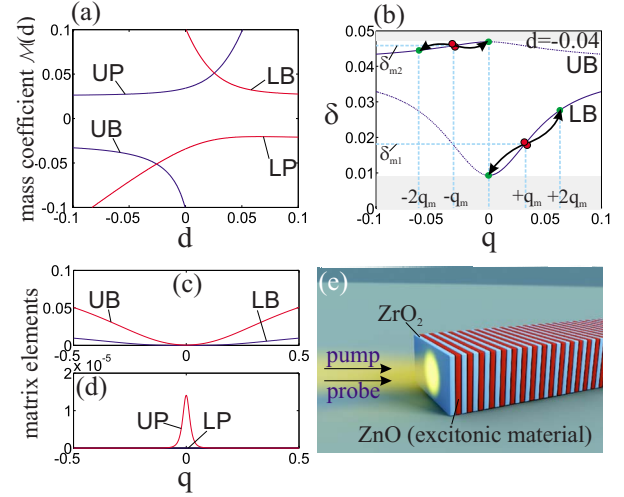


FIG. 3. (Color online) (a) Effective polariton mass parameter \mathcal{M}_j for all branches (indicated) as a function of d . (b) Schematics of the parametric amplification process occurring in the proximity of the inflection points of both Braggordon branches, for $d = -0.04$. Gray areas indicate the photonic subgaps. (c) Matrix element for the intraband parametric scatterings shown in (b), for the LB branch in blue (dark gray) line and for the UB branch in red (light gray) line. (d) Same as (c) but for the LP branch in blue (dark gray) line and for the UP branch in red (light gray) line. (e) Sketch of our proposed design for a polaritonic Bragg stack. The excitonic material is ZnO (shown in red/gray, $\lambda_x = 367.4$ nm), while the second material is ZrO_2 (shown in blue/light gray).

dium and the light field to approximately an order of magnitude, it is possible to achieve low-light-level nonlinear optics.¹⁹ This will open up alternative routes for slow-light-enhanced nonlinearities in gratings.

We have calculated that the physical effective polariton masses at $q = 0$ for each dispersive branch m_j are given by

$$m_j = \frac{\hbar \pi \sqrt{\epsilon_b}}{2c\lambda_x} \mathcal{M}_j(d), \quad (5)$$

where $\mathcal{M}_j(d) \equiv [(\partial^2 \delta_j / \partial q^2)]_{q=0}^{-1}$ is a d -dependent coefficient shown in Fig. 3(a). The prefactor $\hbar \pi \sqrt{\epsilon_b} / (2c\lambda_x)$ assumes the value of $\approx 4 \times 10^{-6} m_e$ for bulk ZnO, which is on the order of magnitude of the cavity photon mass in the upper polariton branch of MCs, with the latter being in practice not usable for nonlinear optics purposes due to the absence of inflection points in the polariton dispersion.¹⁷ Thus 1D polaritonic gratings allow the possibility to obtain very small polariton masses compared to the lower branch of conventional MC polaritons (the mass of which is $\sim 10^{-4} m_e$).¹⁷

Owing to their excitonic content, Braggordons are very nonlinear due to the strong interactions of their constituents, thus giving rise to strong optical nonlinearities of Kerr (cubic) type. The nonlinear coefficient at the exciton resonance can be *several orders of magnitude larger than the one for highly nonlinear optical fibers*.¹⁵ We report here that, by keeping the excitonic nonlinear terms of the PCMEs in Eqs. (3) and (4), a stimulated parametric scattering process occurs for Braggordon states, which is the analog of the parametric amplification in semiconductor MCs originally proposed and

demonstrated in 2000 by Savvidis and co-workers.¹⁸ In this experiment, when an intense pump excites the lower MC polariton branch at a certain “magic angle” (corresponding to a magic wave number, located near the inflection point), one observes a large amplification of a weak probe beam which stimulates the same MC lower branch at normal incidence. Such an amplification is due to the scattering of the two pumped polariton states into a pair of signal and idler polaritons,¹⁸ which follows from the phase-matching conditions (energy and momentum conservation). Only modulationally unstable frequencies can grow rapidly enough to produce the exponential amplification of the weak probe (located at $q=0$) at the expense of the pump. In our system, the phase-matching condition is provided by the nonlinear terms in Eqs. (3) and (4) and is satisfied in close proximity to *two* inflection points [located in the UB and LB branches as shown in Figs. 2(a) and 2(b)]—note that only *one* inflection point is available in MC polaritons—thus effectively giving rise to amplification of Braggoriton states at $q=0$. As we are dealing with a grating structure, these two inflection points can be externally excited just by changing the frequencies of the input pump and probe pulses [see also Figs. 3(b) and 3(e)]. Hence, Braggoriton amplification is characterized by two magic frequencies [δ_{m_1, m_2} in Fig. 3(b)], in correspondence of which one transfers polaritons from the pump ($q=q_m$) to states with $q=0$ [see Fig. 3(b)]. The final states are located symmetrically in both frequency and wave-number spaces.

The scattering processes on the various dispersion branches can have very different matrix elements, and thus the efficiency can vary considerably for different branches, as shown in Figs. 3(c) and 3(d). The intraband matrix elements of the UP and LP branches are shown in Fig. 3(d).

They are negligible for small values of $|d|$, as they are not phase matched, and thus the efficiency of the scattering process on these branches is very low. The opposite scenario is observed for the UB and LB branches [see Fig. 3(c)]. As a typical example, when $d=-0.04$, at a value of $|q| \approx 0.38$, where the zero GVD points are located, the ratio between the matrix element for the UB branch and the one for the LB branch is approximately $r_{UB/LB} \equiv |M_{UB}/M_{LB}| \approx 6$, so that the UB branch is six times “more nonlinear” than the LB branch for the specific material parameters chosen. This ratio can be tuned up by several orders of magnitude by just increasing the value of $|d|$. For instance, for $d=-0.2$ we would have $r_{UB/LB} \approx 2 \times 10^3$ at the zero GVD points. This allows a very large tunability of the effective nonlinearity of the various branches in polaritonic gratings.

In conclusion, we have studied some nonlinear properties of 1D Bragg gratings, when the PBG is near resonant with an excitonic feature of the medium. We have developed a model based on a set of coupled-mode equations [Eqs. (1)–(4)] that are able to accurately describe the linear and the nonlinear propagations of Braggoriton states, which will be instrumental for future theoretical investigations. The crucial feature of such gratings is the existence of two inflection points in the dispersion characteristics, leading to the formation of regions of slow-light-enhanced nonlinear propagation, as well as the establishment of a strong parametric amplification at two magic frequencies. This places the linear and the nonlinear properties of Braggoritons in between those of standard non-resonant Bragg photons and MC polaritons.

F.B. is supported by the German Max Planck Society for the Advancement of Science (MPG). C.C. acknowledges Fondazione CARIPLO for financial support.

¹E. Yablonovitch, Phys. Rev. Lett. **58**, 2059 (1987); S. John, *ibid.* **58**, 2486 (1987).

²A. Yu. Sivachenko, M. E. Raikh, and Z. V. Vardeny, Phys. Rev. A **64**, 013809 (2001).

³N. Eradat, A. Y. Sivachenko, M. E. Raikh, Z. V. Vardeny, A. A. Zakhidov, and R. H. Baughman, Appl. Phys. Lett. **80**, 3491 (2002).

⁴R. Schmidt-Grund, B. Rheinländer, C. Czekalla, G. Benndorf, H. Hochmut, A. Rahm, M. Lorenz, and M. Grundmann, Superlattices Microstruct. **41**, 360 (2007); R. Schmidt-Grund, B. Rheinländer, C. Czekalla, G. Benndorf, H. Hochmuth, M. Lorenz, and M. Grundmann, Appl. Phys. B: Lasers Opt. **93**, 331 (2008); C. Sturm, H. Hilmer, R. Schmidt-Grund, C. Czekall, J. Sellmann, J. Lenzner, M. Lorenz, and M. Grundmann, J. Vac. Sci. Technol. B **27**, 1726 (2009).

⁵M. V. Erementchouk, L. I. Deych, and A. A. Lisyansky, Phys. Rev. B **73**, 115321 (2006).

⁶S. Nojima, Phys. Rev. B **59**, 5662 (1999).

⁷D. Gerace and L. C. Andreani, Phys. Rev. B **75**, 235325 (2007).

⁸L. C. Andreani, in *Electron and Photon Confinement in Semiconductor Nanostructures*, edited by B. Deveaud, A. Quattropani, and P. Schwendimann (IOS Press, Amsterdam, 2003), p. 105.

⁹C. Martijn de Sterke and J. E. Sipe, Prog. Opt. **33**, 203 (1994).

¹⁰C. Ciuti, P. Schwendimann, B. Deveaud, and A. Quattropani, Phys. Rev. B **62**, R4825 (2000); C. Ciuti, P. Schwendimann, and

A. Quattropani, Semicond. Sci. Technol. **18**, S279 (2003).

¹¹F. Médard *et al.*, Photonics Nanostruct. Fundam. Appl. **7**, 26 (2009).

¹²Ü. Özgür, Ya. I. Alivov, C. Liu, A. Teke, M. A. Reshchikov, S. Doğan, V. Avrutin, S.-J. Cho, and H. Morkoç, J. Appl. Phys. **98**, 041301 (2005).

¹³S. F. Chichibu, T. Ohmori, N. Shibata, and T. Koyama, Appl. Phys. Lett. **88**, 161914 (2006).

¹⁴K. Hazu, T. Sota, S. Adachi, S. Chichibu, G. Cantwell, D. C. Reynolds, and C. W. Litton, J. Appl. Phys. **96**, 1270 (2004).

¹⁵W. Zhang, H. Wang, K. S. Wong, Z. K. Tang, G. K. L. Wong, and R. Jain, Appl. Phys. Lett. **75**, 3321 (1999).

¹⁶A. E. Kozhokin, G. Kurizki, and B. A. Malomed, Phys. Rev. Lett. **81**, 3647 (1998); T. Opatrny, B. A. Malomed, and G. Kurizki, Phys. Rev. E **60**, 6137 (1999); E. V. Kazantseva and A. I. Maimistov, Phys. Rev. A **79**, 033812 (2009).

¹⁷A. Kavokin *et al.*, *Microcavities* (Oxford University Press, Oxford, UK, 2007).

¹⁸P. G. Savvidis, J. J. Baumberg, R. M. Stevenson, M. S. Skolnick, D. M. Whittaker, and J. S. Roberts, Phys. Rev. Lett. **84**, 1547 (2000); R. M. Stevenson, V. N. Astratov, M. S. Skolnick, D. M. Whittaker, M. Emam-Ismael, A. I. Tartakovskii, P. G. Savvidis, J. J. Baumberg, and J. S. Roberts, *ibid.* **85**, 3680 (2000).

¹⁹See the focus issue on slow light, Nat. Photonics **2**, 447 (2008).